

Mg acceptor level in InN epilayers probed by photoluminescence

N. Khan, N. Nepal, A. Sedhain, J. Y. Lin, and H. X. Jiang^{a)}

Department of Physics, Kansas State University, Manhattan, Kansas 66506-2601

(Received 6 April 2007; accepted 7 June 2007; published online 2 July 2007)

Mg-doped InN epilayers were grown on sapphire substrates by metal organic chemical vapor deposition. Effects of Mg concentration on the photoluminescence (PL) emission properties have been investigated. An emission line at ~ 0.76 eV, which was absent in undoped InN epilayers and was about 60 meV below the band-to-band emission peak at ~ 0.82 eV, was observed to be the dominant emission in Mg-doped InN epilayers. The PL spectral peak position and the temperature dependent emission intensity corroborated each other and suggested that the Mg acceptor level in InN is about 60 meV above the valance band maximum. © 2007 American Institute of Physics. [DOI: 10.1063/1.2753537]

In recent years, research interest in indium nitride (InN) has significantly increased due to the confirmation of its small band gap energy of ~ 0.62 – 0.7 eV (Refs. 1–9) and its potential applications in semiconductor devices, such as light emitting diodes, laser diodes, high efficiency solar cells, and high performance electronic devices, and in the telecommunications wavelength region ($1.55 \mu\text{m}$).^{10–12} Achieving *p*-type conduction in InN and high In content InGaN alloys is essential for many device applications but has been exceedingly difficult due to the fact that as-grown InN epilayers are generally highly *n* type. There has been strong evidence that InN contains an electron accumulation layer on its surface.⁴ Thus even if *p*-type conductivity in bulk InN is achieved by Mg doping, its surface will remain highly *n* type which creates difficulties in the demonstration of *p*-type InN, as electrical measurements are often dominated by surface *n*-type conducting layers.^{13,14}

Compared to Mg-doped GaN, very few studies have been done so far concerning the basic properties of Mg-doped InN.^{15–18} A previous study using x-ray absorption fine structure analysis suggested that Mg atoms occupy either the In metal (Mg_{In}) or the interstitial (Mg_{InN}) site; Hall effect measurements, however, revealed a *n*-type behavior.¹⁶ More recently, the evidence of a buried *p*-type layer in Mg doped InN was provided by capacitance-voltage (*CV*) measurements.¹⁷ Further evidence of a buried *p* layer beneath a surface electron accumulation layer in heavily Mg-doped InN was provided by variable magnetic field Hall effect and *CV* measurements, from which an energy level of about 110 meV was suggested for the Mg acceptors in InN.¹⁸ So far, detailed studies concerning the optical transitions and the Mg acceptor energy level in Mg-doped InN have not been possible due to the fact that most Mg-doped InN films exhibit no (or weak) photoluminescence (PL) emission.

In this letter, we report on the growth and PL emission characteristics of Mg-doped InN epilayers grown on sapphire substrates by metal organic chemical vapor deposition (MOCVD). Effects of the Mg flow rate (R_{Mg}) on the PL emission properties of Mg-doped InN epilayers have been investigated by varying R_{Mg} from 8.5 to 60 ml/min, corresponding to Mg doping concentration of 1.8×10^{20} – $1.3 \times 10^{21} \text{ cm}^{-3}$. The PL spectroscopy system

consists of a 100 fs Ti:sapphire laser ($\lambda_{\text{exc}}=780 \text{ nm}$), a 0.3 m monochromator, and an InGaAs detector. Electrical properties of Mg-doped InN epilayers were examined by Hall effect measurement. X-ray diffraction (XRD) was employed to study the crystalline quality of Mg-doped InN.

The 0.2 μm thick Mg-doped InN epilayers were grown by MOCVD on sapphire (0001) substrates with 1.5 μm thick GaN epilayer templates. Trimethylindium, trimethylgallium, and NH_3 were used as In, Ga, and N sources, respectively. For Mg doping, bis-cyclopentadienylmagnesium (CP_2Mg) was transported into the growth chamber during InN growth. Atomic force microscopy revealed a root mean square (rms) of surface roughness of about 25–30 nm on a $10 \times 10 \mu\text{m}^2$ area scan, which was comparable to that of undoped InN. The surface morphology started to deteriorate when R_{Mg} exceeded 35 ml/min. Both undoped and Mg-doped InN films were shown to be single crystals based on XRD measurements with a *c* spacing of around 0.568 nm. The full width at half maximum (FWHM) of the rocking curve of the (0002) plane of undoped (Mg-doped) InN epilayers was ~ 500 – 540 (550–630) arc sec. Hall effect measurement was attempted to measure the conductivity of Mg-doped InN epilayers. Complete electron compensation by Mg acceptors could not be observed. Instead, increasing the Mg flow rate from 8.5 to 60 ml/min reduced the free electron concentration (*n*) from 2×10^{19} to $3 \times 10^{18} \text{ cm}^{-3}$ and the *n*-type conductivity (σ) from 1250 to 125 ($\Omega \text{ cm}$)⁻¹ upon postgrowth thermal annealing at 500 °C for 4 min. However, due to the presence of the surface electron accumulation layer, the effects of postgrowth thermal annealing process in Mg doped InN epilayers seem rather complicated and remain to be understood. Furthermore, the postgrowth thermal annealing process may also alter the profile of the surface electron accumulation layer. In order to avoid the complications caused by the postgrowth thermal annealing process in data analysis, we have carried out systematic comparison studies only for unannealed samples, which were shown by the Hall effect measurement to have a comparable free electron concentration.

Figure 1 shows 10 K PL spectra of a set of Mg-doped InN grown under different R_{Mg} where the PL spectrum of an undoped InN epilayer is also included for comparison. The dominant PL emission peak is at 0.82 eV in the undoped InN epilayers, which is higher than the recently reported band gap of InN (0.62–0.7 eV).^{1–9} This spectral blueshift has

^{a)}Electronic mail: jiang@phys.ksu.edu

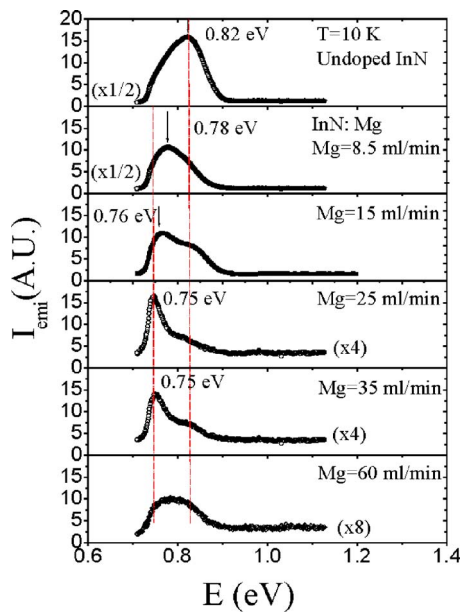


FIG. 1. 10 K PL spectra of Mg doped InN epilayers grown under different Mg flow rates (R_{Mg}). PL spectrum of an undoped InN epilayer is also included for comparison. All samples are unannealed.

been previously observed in both optical absorption^{19,20} and PL spectra of InN (Refs. 20–22) and can be accounted for by the fact that the electron Fermi level (E_F) is above the conduction band minimum or the so-called Moss-Burstein blueshift, which was observed to increase with an increase of the free electron concentration.^{19–22} With respect to the conduction band minimum, E_F can be written as $E_F = \hbar^2/2m^* (3\pi^2 n/v_D)^{2/3}$,²³ where v_D is the degeneracy factor which is 2 for this case, and n and m^* are the electron concentration and electron effective mass, respectively. Using $m^* \sim 0.11m_0$ (Ref. 24) and $n = (1.9–2.0) \times 10^{19} \text{ cm}^{-3}$ for undoped InN, we obtained $E_F = 140–150 \text{ meV}$. Based on this and the room temperature spectral peak position of about 0.80 eV observed in the undoped InN, the band gap of InN is thus deduced to be 0.66–0.65 eV which is in reasonable agreement with the previously reported band gap of InN ($\sim 0.62–0.7 \text{ eV}$). We thus label the 0.82 eV emission line as the band-to-band emission line in InN.

Compared to the undoped InN layer, an additional emission line at $\sim 0.76 \text{ eV}$ emerges and is the dominant emission line in Mg-doped InN epilayers. Since this 0.76 eV emission line is absent in undoped InN, we attribute it to the Mg-related line. This Mg-related emission line is about 60 meV below the band edge emission line at 0.82 eV. Figure 2 summarizes the influence of R_{Mg} on the PL emission properties of the Mg-related line in terms of (a) the spectral peak position E_p , (b) linewidth FWHM, and (c) the intensity ratio of the Mg-related emission line to the band edge emission line. Both E_p and FWHM initially decrease with increasing R_{Mg} up to 25 ml/min and then increase. A similar trend is seen for the band-to-band emission line at 0.82 eV. The spectral blueshift seen for $R_{Mg} > 25 \text{ ml/min}$ could be due to an increase in the incorporation of defects and impurities at higher R_{Mg} that increase n and E_F .²⁵ The integrated emission intensity (I_{emi}) of the Mg-related transition is observed to decrease exponentially with increasing Mg doping concentration, following a similar trend as the Mg-related transition line in Mg-doped GaN.²⁶ However, the relative intensity of the Mg-

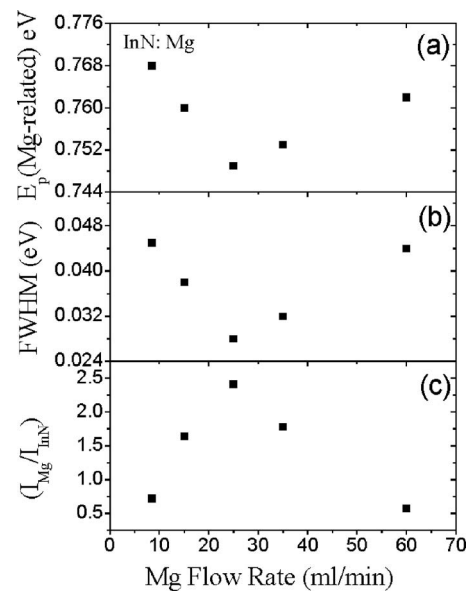


FIG. 2. Variations of the (a) spectral peak position E_p , (b) full width at half maximum (FWHM), and (c) intensity ratio of the Mg-related emission line to the band-to-band transition line with the Mg flow rate R_{Mg} . All samples are unannealed.

related emission line to the band-to-band emission line exhibits a maximum at $R_{Mg} = 25 \text{ ml/min}$, as shown in Fig. 2(c).

Figure 3 presents the PL spectra measured at different temperatures for the Mg-doped InN epilayer grown under $R_{Mg} = 15 \text{ ml/min}$. The spectral peak separation of about 60 meV between the Mg-related and band-to-band emission lines is clearly measured at $T < 100 \text{ K}$. At $T > 100 \text{ K}$, only the Mg-related emission line can be resolved. Both emission lines exhibit a blueshift with increasing temperature. This blueshift with temperature is in a sharp contrast to the temperature dependence of the direct band gap (E_g) in most semiconductors, in which a reduction of E_g with increasing

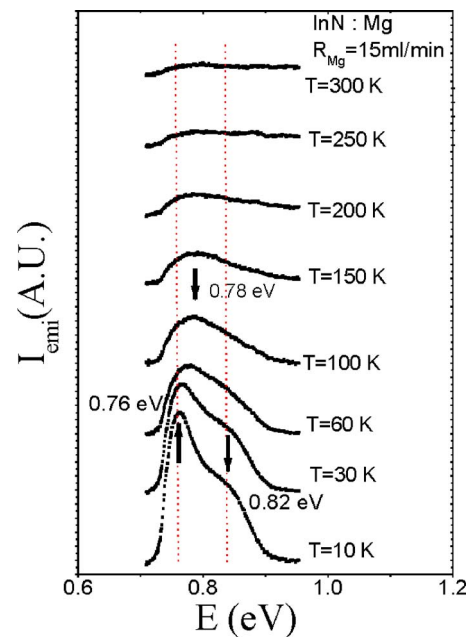


FIG. 3. PL spectra of Mg doped InN grown under the Mg flow rate $R_{Mg} = 15 \text{ ml/min}$, measured at different temperatures. All samples are unannealed.

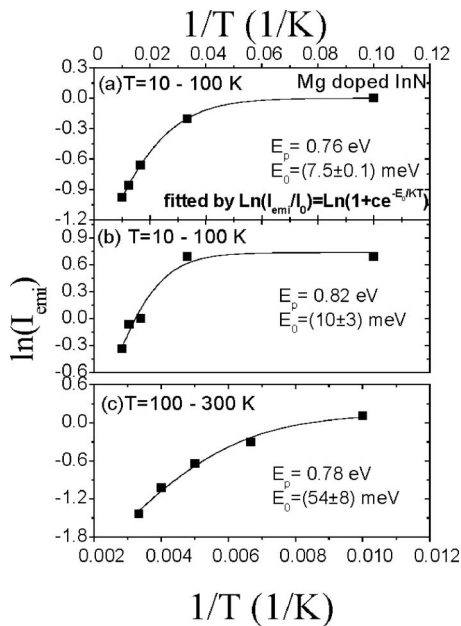


FIG. 4. The Arrhenius plots of the PL emission intensity, $\ln(I_{\text{emi}})$ vs $1/T$, for (a) the Mg-related emission line measured in the temperature range of $T=10\text{--}100$ K, (b) the band edge emission line measured in the temperature range of $T=10\text{--}100$ K, and (c) the Mg-related emission line measured at $T=100\text{--}300$ K. The fitted activation energies (E_0) are indicated in the figure. All samples are unannealed.

temperature is typically observed. The spectral blueshift with temperature may be caused by the electron Fermi level increase due to the free electron concentration increase at higher temperatures.^{1,27} This interpretation is also supported by the Hall effect measurement result that revealed a linear increase of the electron concentration with temperature.

The Arrhenius plots of PL emission intensities (I_{emi}) measured in different temperature ranges for Mg-doped InN with $R_{\text{Mg}}=15$ ml/min are shown in Fig. 4. The solid lines are the least squares fit of the data with equation $I_{\text{emi}}(T)=I_0/[1+C \exp(-E_0/KT)]$, where E_0 is the activation energy of I_{emi} . The Arrhenius plots in the temperature range of 10–100 K, as shown in Figs. 4(a) and 4(b), yield activation energies of 7.5 and 10 meV, respectively, for the Mg-related emission line and the band-to-band emission line, which may be accounted for by the existence of nonradiative recombination channels.^{12,21} In the temperature range of 100–300 K, the activation process is governed by an activation energy of 54 meV. This activation energy coincides fairly well with the spectral peak energy difference of about 60 meV between the Mg-related and the band-to-band transition lines. We therefore believe that the Mg acceptor energy level in InN is about 60 meV above the valance band maximum. The Mg acceptor binding energy of 60 meV in InN obtained from our present work matches well with a recently reported value of about 62 meV observed in Mg-doped InN epilayers grown by molecular beam epitaxy.²⁸

In summary, we have grown by MOCVD and studied the PL emission characteristics of Mg-doped InN epilayers. An emission line of about 60 meV below the band-to-band emission, which was absent in undoped InN epilayers, was ob-

served in Mg-doped InN. Together with the temperature dependent PL emission intensity result, we suggest that the Mg acceptor level in InN is about 60 meV above the valance band maximum.

This work was supported by NSF (DMR-0504610) and AFOSR (FA9550-06-1-0441).

- ¹J. Wu, W. Walukiewicz, K. M. Yu, J. W. Ager, III, E. E. Haller, H. Lu, W. J. Schaff, Y. Saito, and Y. Nanishi, *Appl. Phys. Lett.* **80**, 3967 (2002).
- ²J. Wu, W. Walukiewicz, K. M. Yu, W. Shan, J. W. Ager, III, E. E. Haller, Hai Lu, W. J. Schaff, W. K. Metzger, and Sarah Kurtz, *J. Appl. Phys.* **94**, 6477 (2003).
- ³S. H. Wei, X. Nie, I. G. Batyrev, and S. B. Zhang, *Phys. Rev. B* **67**, 165209 (2003).
- ⁴I. Mahboob, T. D. Veal, C. F. McConville, H. Lu, and W. J. Schaff, *Phys. Rev. Lett.* **92**, 036804 (2004).
- ⁵W. Walukiewicz, *Physica E (Amsterdam)* **20**, 300 (2004).
- ⁶S. X. Li, K. M. Yu, J. Wu, R. E. Jones, W. Walukiewicz, J. W. Ager, III, W. Shan, E. E. Haller, Hai Lu, and William J. Schaff, *Phys. Rev. B* **71**, 161201(R) (2005).
- ⁷P. Carrier and S. H. Wei, *J. Appl. Phys.* **97**, 033707 (2005).
- ⁸S. P. Fu, T. T. Chen, and Y. F. Chen, *Semicond. Sci. Technol.* **21**, 244 (2006).
- ⁹W. Walukiewicz, J. W. Ager, K. M. Yu, Z. Liliental-Weber, J. Wu, S. X. Li, R. E. Jones, and J. D. Delinger, *J. Phys. D* **39**, R38 (2006).
- ¹⁰A. G. Bhuiyan, A. Hashimoto, and A. Yamamoto, *J. Appl. Phys.* **94**, 2779 (2003).
- ¹¹M. C. Johnson, S. L. Konsek, A. Zettl, and E. D. Bourret-Courchesne, *J. Cryst. Growth* **272**, 400 (2004).
- ¹²R. Intartagilla, B. Maleyre, S. Ruffenach, O. Briot, T. Taliercio, and B. Gil, *Appl. Phys. Lett.* **86**, 142104 (2005).
- ¹³V. Camilla, M. Niebelschutz, G. Ecke, V. Lebedev, O. Ambacher, M. Himmerlich, S. Krischok, J. A. Schaefer, H. Lu, and W. J. Schaff, *Phys. Status Solidi A* **203**, 59 (2006).
- ¹⁴V. Cimalla, M. Niebelschutz, G. Ecke, O. Ambacher, R. Goldhahn, H. Lu, and W. J. Schaff, *Phys. Status Solidi C* **3**, 1721 (2006).
- ¹⁵V. V. Mamutin, V. A. Vekshin, V. Yu. Davydov, V. V. Ratnikov, Yu. A. Kudriavtsev, B. Ya. Ber, V. V. Emtsev, and S. V. Ivanov, *Phys. Status Solidi A* **176**, 373 (1999).
- ¹⁶A. V. Blant, T. S. Cheng, N. J. Jeffs, L. B. Flannery, I. Harrison, J. F. W. Mosselmann, A. D. Smith, and C. T. Foxen, *Mater. Sci. Eng., B* **59**, 218 (1999).
- ¹⁷R. E. Jones, K. M. Yu, S. X. Li, W. Walukiewicz, J. W. Ager, E. E. Haller, H. Lu, and W. J. Schaff, *Phys. Rev. Lett.* **96**, 125505 (2006).
- ¹⁸P. A. Anderson, C. H. Swartz, D. Carder, R. J. Reeves, S. M. Durbin, S. Chandril, and T. H. Myers, *Appl. Phys. Lett.* **89**, 184104 (2006).
- ¹⁹J. Wu, W. Walukiewicz, S. X. Li, R. Armitage, J. C. Ho, E. R. Weber, E. E. Haller, Hai Lu, William J. Schaff, A. Barcz, and R. Jakiela, *Appl. Phys. Lett.* **84**, 2805 (2004).
- ²⁰K. Sugita, H. Takatsuka, A. Hashimoto, and A. Yamamoto, *Phys. Status Solidi B* **240**, 421 (2003).
- ²¹G. W. Shu, P. F. Wu, M. H. Lo, J. L. Shen, T. Y. Lin, H. J. Chang, Y. F. Chen, C. F. Shih, C. A. Chang, and N. C. Chen, *Appl. Phys. Lett.* **89**, 131913 (2006).
- ²²M. Higashiwaki, T. Inushima, and T. Matsui, *Phys. Status Solidi* **240**, 417 (2003).
- ²³K. W. Boer, *Survey of Semiconductor Physics: Electrons and other Particles in Bulk Semiconductors* (Van Nostrand Reinhold, New York, 1990), p. 240.
- ²⁴S. P. Fu and Y. F. Chen, *Appl. Phys. Lett.* **85**, 1523 (2004).
- ²⁵S. X. Li, R. E. Jones, E. E. Haller, K. M. Yu, W. Walukiewicz, J. M. Ager, Z. L. Weber, H. Lu, and W. J. Schaff, *Appl. Phys. Lett.* **88**, 151101 (2006).
- ²⁶M. Lachab, D.-H. Youn, R. S. Qhalid Fareed, T. Wang, and S. Sakai, *Solid-State Electron.* **44**, 1669 (2000).
- ²⁷F. Chen, A. N. Cartwright, H. Lu, and W. J. Schaff, *Physica E (Amsterdam)* **20**, 308 (2004).
- ²⁸X. Wang, S. B. Che, Y. Ishitani, and A. Yoshikawa, *Appl. Phys. Lett.* **90**, 201913 (2007).